Digest Journal of Nanomaterials and Biostructures Vol. 9, No. 4, October - December 2014, p. 1513 - 1522

ON THE TRANSPORT PHENOMENA IN HIGHLY IONIZED PULSED PLASMA DURING FeCuNbSiB THIN FILM DEPOSITION PROCESS

I. L. VELICU, V. TIRON*
Faculty of Physics, Alexandru Ioan Cuza University, 700506, Iasi, Romania

The transport of sputtered particles in a magnetron discharge is of considerable interest for optimizing the deposition technique with respect to both deposition rate and control of the thin film properties. The High Power Impulse Magnetron Sputtering (HiPIMS) is a relatively new sputtering-based ionized physical vapor deposition technique with high density and high ionization degree of sputtered atoms which offers favorable conditions for better control and high-quality growing of thin films. Operating the HiPIMS in short pulse mode allows increasing the deposition rate due to the reduced gas rarefaction effect and reducing the ion back-attraction of the ionized sputtered material. Results concerning the spatial and temporal evolution of both the sputtered atoms density and plasma potential, the temporal evolution of the ion current intensity recorded by an electrostatic probe placed close to the substrate and the total positive electrical charge collected by the target and the probe during $Fe_{73.5}Cu_1Nb_3Si_{15.5}B_7$ thin film deposition process are presented. Most of the depositions and investigations have been made for a constant pulse voltage value of -1 kV, short pulse durations (4-20 μs), 10 mTorr working gas pressure and 30 W average power.

(Received October 1, 2014; Accepted November 24, 2014)

Keywords: Pulsed magnetron sputtering, Plasma diagnostics, FeCuNbSiB thin films.

1. Introduction

It is already well known that the magnetron sputtering is a powerful and versatile tool for thin films deposition. In both sputtering and deposition process, the properties of the deposited films are dependent on the: interaction between the arriving particles and the substrate, sputtering and deposition rates, energy and the mobility of the sputtered particles at the substrate surface and substrate temperature [1].

The High Power Impulse Magnetron Sputtering (HiPIMS) is a relatively newly developed plasma-based vapor deposition technique whose main feature is to provide high pulse power densities at very low duty cycles. Over the last few years, this technology became a significant opportunity for growing high-quality thin films for a wide variety of electronic and industrial applications. The high ionization degree allows obtaining smooth and dense films and improves the adhesion to the substrate. The increasing probability for ionizing collisions and, therefore, the plasma enriched with large quantities of ionized sputtered material, make the flux of ions more important in the films growing process in comparison with the case of conventional magnetron sputtering. Consequently, the electric field within the plasma volume plays an important role in both ion kinetic and transport processes. Undoubtedly, it should not be excluded that the properties of the deposited films are also highly dependent on the sputtered atoms arrived at the substrate level [2-6].

Providing a unique combination of superior soft magnetic properties, amorphous and nanocrystalline FeCuNbSiB alloys (ribbons, wires, thin films, etc.) have attracted considerable scientific and technological interest. One method for achieving the nanocrystalline state is subjecting the amorphous precursor to adequate thermal treatments [8, 9]. FeCuNbSiB amorphous

* Corresponding author: vasile.tiron@uaic.ro

thin films can be grown by various physical deposition techniques. Previous works showed that the HiPIMS technique allows obtaining amorphous FeCuNbSiB thin films with coercivities up to two orders of magnitude smaller than those of the films with the same thickness and composition deposited through other techniques [10]. It has also been shown that, for the same average power, the deposition rate of this type of alloy decreases about 30% when the pulse duration increases from 4 μs to 20 μs [10, 11].

The aim of this paper is to investigate both transport phenomena and kinetics process of neutrals (atoms) and charged particles (ions) within the plasma volume during the deposition process of FeCuNbSiB thin films, as well as the time and space evolution of the plasma potential. The provided information may serve to establish the optimum deposition conditions for obtaining amorphous FeCuNbSiB thin films with improved soft magnetic properties, as well as to better understand some processes occurring during the deposition process.

2. Experimental details

Amorphous FeCuNbSiB thin films have been deposited onto glass substrates using the HiPIMS technique. The depositions were performed under pure argon atmosphere (constant working gas flow rate of 20 sccm), using an unbalanced planar circular magnetron source equipped with a disk-shaped target (diameter of 5.6 cm) made by multiple ribbons with the nominal composition $Fe_{73.5}Cu_1Nb_3Si_{15.5}B_7$ (Vacuumschmelze GmbH). The parallel component of the magnetic field to the cathode surface was about 1000 Gauss. The substrates were axially placed at 6 cm above and parallel to the cathode surface [11]. The pulse voltage was set to a constant value of about -1 kV for very short pulses (4-20 μs), achieving a target current density of several amperes per square centimeter, giving rise to a very dense plasma in the race track region. The average discharge power was varied in the range of 30-90 W, but most of the depositions and investigations have been made for 10 mTorr working gas pressure and 30 W average power. These conditions were indicated by previous works as optimum deposition conditions for obtaining amorphous $Fe_{73.5}Cu_1Nb_3Si_{15.5}B_7$ thin films with good soft magnetic properties and smooth and uniform surfaces [10].

The surface chemical composition of the films was analyzed by X-ray photoelectron spectroscopy (XPS), using a PHI 500 VersaProbe spectrometer.

The pulse voltage was monitored by a 1:100 voltage probe (TesTec) connected to the cathode feed-through. The pulse duration and repetition rate have been set by the pulse unit. The current probe was integrated directly into the pulsing system and calibrated by a commercial large bandwidth probe.

In order to study the temporal and spatial evolution of the sputtered iron atoms, Tunable Diode – Laser Absorption Spectroscopy (TD-LAS) measurements were performed using a Toptica Photonics DL 100 system with a tunable single-mode diode laser, centered at $\lambda_0 = 407.174$ nm. This wavelength corresponds to the neutral Fe transition from the metastable level $3d^7(^4F)4s$ to the radiative excited level $3d^7(^4F)4p$. The laser beam probes the plasma volume in a parallel direction to the target, at different axial distances from the target surface (from 0.5 to 50 mm).

The temporal and spatial evolution of the plasma potential, in axial direction from the target surface to the substrate, above the race-track, was monitored using an emissive probe with 10 ns time-resolution. The measurements were made at every 5 mm outside the magnetic trap ($10\,\text{mm} < z < 55\,\text{mm}$) and at every 1 mm inside the magnetic trap ($2\,\text{mm} < z < 10\,\text{mm}$). The emissive probe consists of thoriated tungsten wire (0.2 mm diameter and 3 mm length), fitted into two bore ceramic tubes provided with copper connecting wires. The plasma exposed tungsten wire has cylindrical shape, its axis being orientated parallel to the target surface. In order to avoid the ground loops and unwanted electrical noises in the circuit, the emissive probe was heated using an insulated battery driven electronic circuit, by which the heating current intensity can be adjusted very accurately. The plasma potential was measured as probe floating potential when the emissive probe was heating to thermal electron emission.

Information on the ion flux at the substrate region were obtained using a cold electrostatic probe (ring shape of 4 cm diameter, made of tungsten wire of 2 mm diameter) with a collecting area of 4 cm^2, axially placed surrounding the emissive probe, at a distance of 8 cm from the cathode discharge. The probe was negatively biased (-100 V) with respect to the anode, using a DC power supply. The time evolution of the probe current intensity during the pulse discharge was stored on the oscilloscope.

3. Results and Discussion

The results to be presented are based on some simplifying approximations. No doubt, each of the chemical elements from the target composition ($Fe_{73.5}Cu_1Nb_3Si_{15.5}B_7$) is involved in the sputtering process, but for this study was taken into account just the predominant element (iron, 73.5 at.%). More than that, for the selected deposition conditions, the XPS results revealed that the composition of the obtained films is very close to the target composition. Consequently, it might be assumed that, during both the sputtering and deposition processes, the other four elements follow the same behaviour and obey same rules as iron.

According to both NIST data on Atomic Spectra Database [12] and Grotrian diagram [13], the lifetime of the metastable level $3d^7(^4F)4s$ is about 8 s, which means that, even if it has a higher energy, it might be considered acting as the ground state. Consequently, even if the obtained results do not provide information about the absolute value of the Fe neutrals density, they might be considered as proportional to it.

Information about the absorbing iron atoms, δN (having a certain velocity in the axial direction), within the plasma volume, δV (defined by the leaser beam cross section and the distance probing the plasma volume), have been obtained by measuring the plasma absorption coefficient k_0 at the resonant wavelength λ_0. This coefficient is proportional to the density of the probed species and is given by Lambert-Beer law [14]:

$$k(\lambda_0)L = -\ln(I_L / I_0) \tag{1}$$

where L is the optic distance of the laser beam probing the plasma volume, I_0 and I_L represent the laser source intensities measured before and after absorption, respectively.

The temporal evolution of the maximum absorption signal at λ_0, during one pulse period, at different axial distances from the cathode surface and different pulse durations was synchronized with the pulsed voltage. The obtained data were grouped into a matrix in which each horizontal line represents the temporal evolution of the maximum absorption signal during one pulse period (for a fixed distance from the cathode surface), while, each reconstructed column represents the spatial evolution of the maximum absorption signal at a fixed time. Consequently, a 2D map contour representation of this matrix illustrates a complete view on both spatial and temporal evolution of the absorbing iron atoms.

Figure 1 (a and b) presents the spatial and temporal evolution of the maximum absorption signal for the cases when the pulse duration value was fixed at 4 μs (Fig. 1a) and 20 μs (Fig. 1b), respectively. These maps provide information about kinetic of the iron sputtered atoms from the target and their spreading in radial and axial directions with larger time spread interval for larger distances from the target. Moreover, the spatial evolution of the maximum absorption coefficient in virtually any instant time on the pulse period can be obtained.

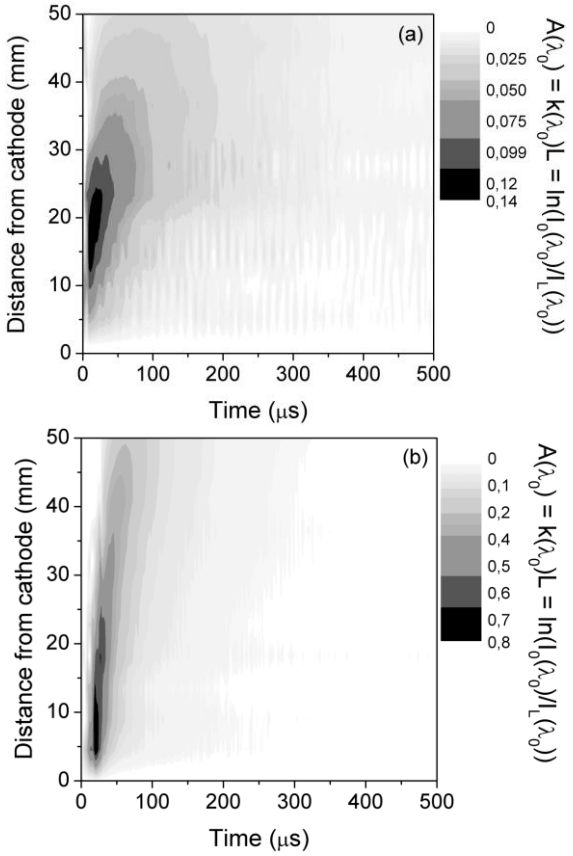

Fig. 1. Absorbance of the metastable iron atoms: temporal and spatial evolution for 4 μs (a) and 20 μs (b) pulse duration.

For the sake of clarity, Figure 2 (a and b) shows the temporal evolution of the maximum absorption coefficient of the iron spectral line (Fig. 2a) for selected distances from the cathode and the spatial evolution (Fig. 2b) of the maximum absorbance at 25 μs and 100 μs after the pulse ignition. All the measurements have been performed for pulse duration of 20 μs.

At first glance, increasing the distance from the target surface, the density of the absorbing iron sputtered atoms rapidly increases. This behaviour is due to the increase of the pulse discharge current intensity and may last a little bit longer than the pulse duration. A possible explanation would be the time of flight of the sputtered atoms necessary to reach the detection region. After reaching a certain maximum value, the density of the iron sputtered atoms rapidly decreases in time due to the exclusively physical processes in the afterglow plasma. This result can be explained by taking into account the results obtained and reported mainly in the steady state regime [15], but also during the pulse [16, 17]. It has been shown that two groups of sputtered atoms have to be considered: an energetic one with a very broad energy spectrum and a thermal one with an average kinetic energy around or a little bit higher than the room temperature. The energetic group has a quasi-ballistic behaviour. There is a high probability that the energetic atoms to collide the buffer gas atoms and to be scattered. But even in these circumstances, a small fraction of them may still reach both the substrate and the chamber walls with rather high kinetic energy values. Close to the target surface, once the power pulse is ended, their number continuously decreases in time. The thermal group has two components: the original low-energy sputtered atoms and the rather-energetic sputtered atoms scattered (in space and velocity) by the buffer gas atoms. The low-energy group has the main contribution in the laser absorption process and it may also explain the maximum of iron atoms in a few mm distance from the target. The time and space behaviour of this thermal group is controlled mainly by diffusion due to the large gradient in both radial and axial directions.

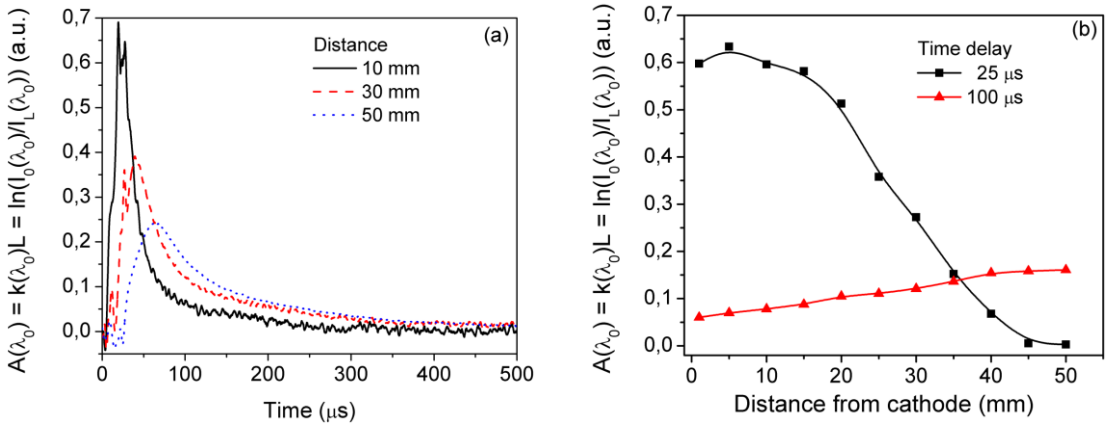

Fig. 2. Maximum absorption coefficient of the iron spectral line: temporal (a) and spatial (b) evolution at selected distances and times.

As it can be seen, both maximum values and decreasing rate of the iron atoms density decrease with increasing distance from the target surface (Fig. 2a). It was noticed that the time decay of the maximum absorption signal is independent on the pulse duration in the range from 4 μs to about 20 μs. By increasing the pulse duration from 4 μs to 20 μs, but maintaining the same average discharge power (30 W), the absorbance maximum (measured at 50 mm above the target) increases about 7 times, while the repetition frequency of the pulse decreases about one order of magnitude. Figure 2b clearly shows the axial distribution of the energetic (time delay of 25 μs) and thermal (time delay of 100 μs) group of the sputtered iron atoms. Increasing the distance from the target, the energetic group becomes thermalized by collision with the buffer gas.

In order to characterize the possible electric field within the plasma volume, which may influence both the ion kinetic and transport processes, the time and space evolution of the plasma potential was investigated. The electric field may act either as a potential barrier to the ionized species or it may accelerate and enhance the ion transport, affecting both the sputtering and deposition rate [18]. Figure 3 (a and b) illustrates the voltage discharge waveform and the time evolution of the plasma potential during one pulse period measured at different positions inside the magnetic trap region for a pulse duration of 20 μs (Fig. 3a) and, for more details, the plasma potential during the pulse (Fig. 3b).

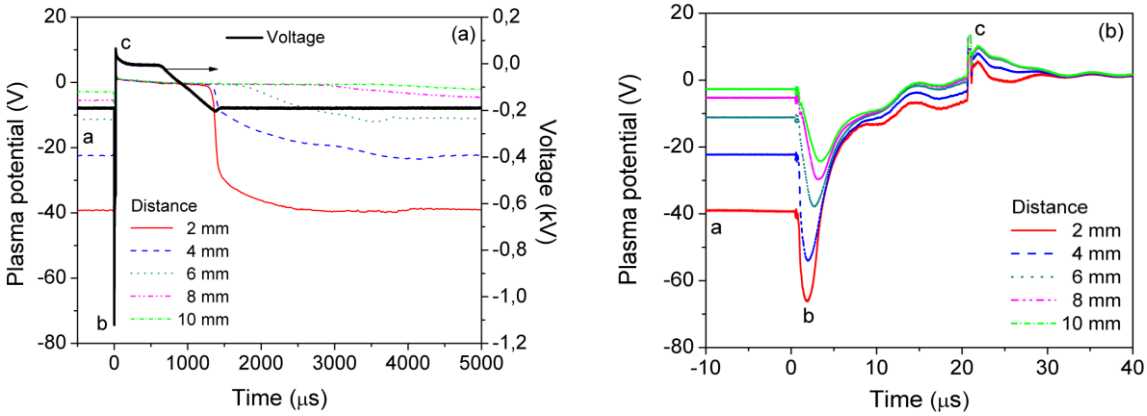

Fig. 3. The time evolution of the plasma potential at selected distances inside the magnetic trap region: during one pulse period (a) and during the pulse (b).

The time evolution of the plasma potential shows three phases labelled in both figures as: (a) – pre-ionization phase, (b) – peak "on-phase" and (c) – peak "off-phase". The plasma potential versus axial distance from cathode, for the three phases, is presented in Figure 4, for pulse durations of 4 μs and 20 μs, respectively.

In the case of 20 μs pulse duration, in the pre-ionization phase, a cathode voltage value of about -200 V was self-adjusted. As it can be seen, in the magnetic trap region, the plasma potential increases from -39 V to -2.5 V. Outside the magnetic trap region, the plasma potential profile is almost flat, a slight increase with the distance (+1 V in the substrate vicinity) being observed.

The measurements performed during the pulse showed a highly dynamic nature of the plasma potential, with negative values up to -70 V at 2 mm distance from cathode and strong potential gradients in the magnetic trap region in the first 2-3 μs after the ignition of the discharge pulse. There is a very slight delay (~1 μs) between the discharge voltage peak and the plasma potential structure formation in the bulk trapped plasma.

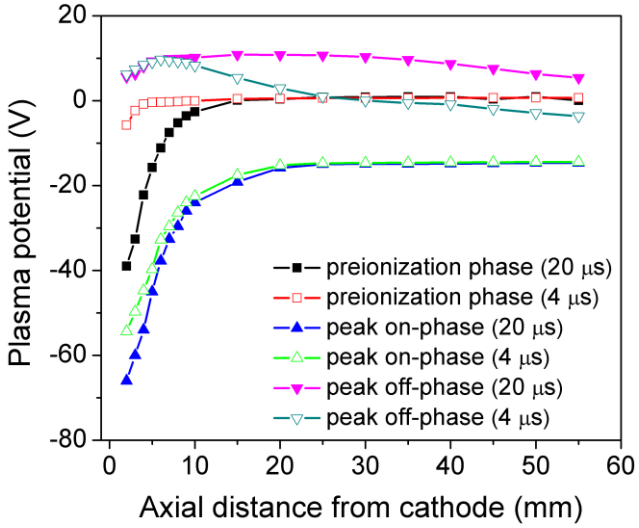

Fig. 4. Plasma potential dependence on the axial distance from the cathode surface for the preionization, peak on– and peak off– phases and two different pulse durations.

The strong plasma potential gradient reveals large axial electric fields, which, close to the target, can reach intensities of the order 8 kVm^{-1}. The large axial electric field, developed in the early stage of the pulse, accelerates the present argon ions produced close to the target in the pre-ionization phase towards the cathode, initiating both the sputtering and secondary electron emission processes. This makes possible very fast onset of the high power pulse and rapidly increase of the discharge current intensity. The plasma potential is always negative during the on-pulse. Its spatial structure in magnetic trap region provides a large potential barrier for the sputtered ionized species, avoiding their transport to the substrate. The sputtered ionized species are back-attracted to the target by the large axial electric field and strongly accelerated in the cathode fall. Outside the magnetic trap region, the plasma potential peak increases very slowly with the distance and the axial electric field is very weak (E ~ 0.1 kVm^{-1}). Therefore, the positive ions produced outside the magnetic trap will "see" a weak axial electric field directed to the discharge chamber, but mainly to the negatively biased substrate. Moreover, at the early stage of the pulse discharge, the ion plasma composition outside the magnetic trap is dominated by the argon ions. In the "off-phase" (afterglow post-high power pulsed discharge), but before pre-ionization phase, the plasma potential goes from above ground potential to about +10 V in the magnetic trap region, its axial distribution showing a slight variation with the distance.

Figure 5 illustrates the time evolution of the ion current intensity collected for different pulse duration (90 W average power).

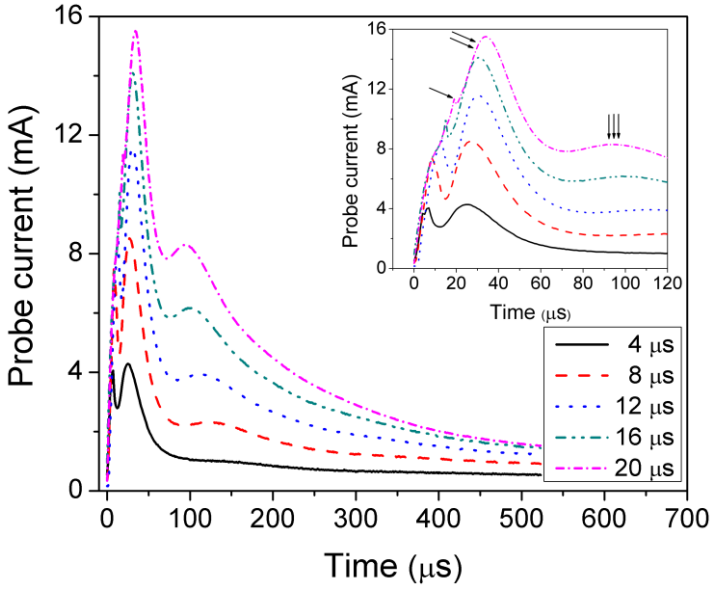

Fig. 5. Temporal evolution of the ion current intensity for selected pulse durations.

The ion flux arrived at the probe lasts much longer time than the discharge pulse. Each waveform shows three distinct peaks. First peak (one arrow) is attributed to the argon ions produced in the early stages of the discharge by the ionization front generated by the fast electron crossing the target to the substrate gap. The second peak (two arrows) corresponds to the ionized ballistic sputtered atoms [19]. The metal ions are mainly generated only after the target current reaches high values and the sputtered atom density in front of the target increases significantly, so that the ionization process of the sputtered atoms becomes dominant. The amount of the metal ions increases with increasing the pulse duration, but not linearly because the probability to be back-attracted by the target also increases with the pulse duration. Moreover, a significant fraction of ions is transported outwards, in radial direction, away from the discharge axis, toward the sidewalls [20, 21], lowering the number of ions traveling forward to the substrate. The average metal ion velocity can be estimated from the time delay of the second peak. The average velocity distribution increases from 2.5 km/s (pulse duration of 20 μs) to 3.5 km/s (pulse duration of 4 μs). At short pulse durations, but higher frequency (in order to maintain the same average power), the plasma conductivity in the after-glow discharge is higher and ion transport from target to probe is improved.

In order to diffuse freely towards the substrate, the target-to-substrate gap must be conductive enough (the space charge density of the metal ions must be compensated by the surrounding electrons). Using the average velocity of the metal ions, the peak metal plasma density can be estimated to about 9×10^{17} m^{-3}. With the knowledge of the film thickness growth rate, which represent the total arrival rate of metal particles (ions and neutral atoms), the roughly estimation of the ionization fraction of sputtered species up to 35% was obtained.

The third peak (three arrows) is the most interesting phenomenon. It was assumed either as an ion acoustic wave reflected off the chamber wall [22] or as a spherically expanding ion-acoustic solitary wave, which do not fit to the simple Korteweg - de Vries model [23]. On the other hand, the thorough analysis made by *Ishihara et al.* [24] shows details on the role of the density and velocity gradient in the reflection mechanism, which has to be also considered in this case. *Alami et al.* [22] pointed out that the ion composition in this peak consists mainly of working gas ions. Higher current intensity and faster emergence of the third peak is achieved increasing the pulse duration and pulse energy. Moreover, *Ehiasarian et al.* [25] have shown a rather complex composition and energy distribution function of various argon and metallic ions within the pulse magnetron discharge. These finding show that more attention has to be paid in understanding the third peak obtained in such highly non homogenous, rather collisional and anisotropic transient

plasma. If the third peak is a "density-wave" initiated during the pulse-on time at the cathode side of the plasma boundary, than it is propagating with a velocity close to the ion-acoustic speed [23]:

$$v_s = \left(\frac{\gamma_i \cdot k \cdot T_i + k \cdot T_e}{M_{Ar}} \right) \tag{2}$$

where k is the Boltzmann constant, γ_i is the adiabatic constant for working gas ($\gamma_i = 3$), M_{Ar} is the molecular mass of the Ar gas, T_i is the ion temperature and T_e is the electron temperature. The TD-LAS measurements made close to the substrate showed the neutral iron temperature is about 400 K. So, considering the iron ion temperature equal to the neutral iron temperature, from Eq. (2) the electron temperature as $T_e = 0.2$ eV can be estimated. The electron temperature value is then used in order to obtain the plasma density n_0 (if ion saturation current is known and using the Bohm sheath criteria). The ions will enter in the sheath at a velocity given by the potential drop across the pre-sheath region, namely Bohm velocity [26]:

$$v_B = \sqrt{\frac{k \cdot T_e}{M_{Ar}}} \,. \tag{3}$$

Assuming that the flux is conserved in the sheath and the ion current is given by [27]:

$$I_{i,sat} = 0.6 \cdot n_0 \cdot e \cdot A \sqrt{\frac{k \cdot T_e}{M_{Ar}}} \tag{4}$$

where A is effective collecting area of the probe, the peak plasma density can be estimated as 3×10^{18} m^{-3}.

The total electrical charge collected by the electrostatic probe was calculated by integrating the aria below the probe ion current waveforms within the full pulse period. The total electrical charge transported to the cathode by the plasma ions was also calculated by integrating the aria below the target current waveforms. During the "off-time", the pre-ionization current is very low and its contribution to the total target current might be neglected. The obtained results are presented in Figure 6.

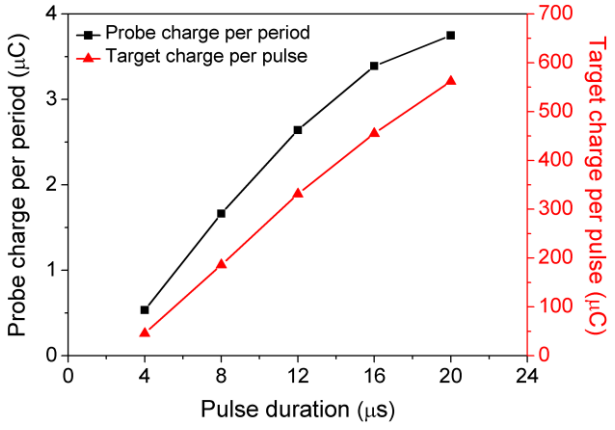

Fig. 6. Total electrical charge collected by the probe and the target, respectively, for different pulse durations.

The total ion charge brought at the cathode during the power pulse increases almost linearly (32 C/s) with the pulse duration. This is nothing else but the discharge current intensity during the pulse and shows a large ionization rate due to the sputtered metallic atoms. Under the

hypothesis that the total current intensity at the cathode is flowing through the race track, the ion charge density arrived at the cathode in a second during the pulse is about $5\,\mathrm{C/cm^2 \times s}$. During the same experiment, the positive electrical charge arrived at the electrostatic probe (placed close to the substrate) increases with the pulse duration and tends to saturate at longer pulse durations. This fact shows two things. First, the decrease of the neutral flux towards the substrate [11], with increasing the pulse duration, for the same mean power transferred to the plasma system, is well compensated by the increase of the ion flux shown in Fig. 6. The second conclusion is that, for longer durations of the power pulse, a tendency for saturation in the transport process of both the ions and neutrals towards substrate may appear. The ratio between the number of ions collected by the probe and the number of ions bombarding the cathode is higher for short pulse durations. This phenomenon is probably due to the change in the plasma properties controlled by the high ionization degree coupled with ion back scattering.

4. Conclusions

The transport phenomena and kinetics process in HiPIMS plasma during $Fe_{73.5}Cu_1Nb_3Si_{15.5}B_7$ thin films deposition process were investigated. The presented results mainly refer to the: temporal and spatial evolution of both maximum absorption signal at $\lambda_0 = 407.174$ nm (proportional to the iron neutral metastable atoms density) and plasma potential, temporal evolution of ion current intensity collected by an electrostatic probe placed close to the substrate, total electrical charge collected by both the target and the probe.

The absorption measurements provided information about the kinetic and the radial/axial spreading of the iron sputtered atoms, offering the possibility of obtaining the spatial evolution of the maximum absorption coefficient in virtually any instant time on the pulse period. Increasing the distance from the cathode, the density of the absorbing iron atoms rapidly increases, reaches a maximum value and then begins to rapidly decrease in time. Both maximum values and decreasing rate of the iron atoms density decrease by increasing the distance from the target.

In the magnetic trap region, the plasma potential presents a highly dynamic nature and strong potential gradients in the first 2-3 μs after the ignition of the discharge pulse, while outside this region its profile becomes almost flat.

The temporal evolution of the ion current intensity collected close to the substrate presents three peaks which can be attributed to the: argon ions produced by the ionization front generated by the fast electron crossing the target to the substrate gap, ionized ballistic sputtered atoms and ion acoustic wave.

During the power pulse, the total ion charge collected by the target increases almost linearly with increasing the pulse duration. The positive electrical charge collected by the electrostatic probe also increases with the pulse duration, tending to saturate at longer pulse durations.

Acknowledgements

This work was supported by UEFISCDI Romania under the grant PN-II-PT-PCCA-2 no. 174/2012.

References

[1] P. J. Kelly, R. D. Arnell, Vacuum **56**, 159 (2000).
[2] P. J. Kelly, J. W. Bradley, J. Optoelectron. Adv. Mater. **11**, 1101 (2009).
[3] J. T. Gudmundsson, N. Brenning, D. Lundin, U. Helmersson, J. Vac. Sci. Technol. A **30**, 030801 (2012).
[4] D. Lundin, K. Sarakinos, J. Mat. Sci. **27**, 780 (2012).

[5] A. Anders, Surf. Coat. Technol. **205**, S1 (2011).

[6] D. Lundin, N. Brenning, D. Jädernäs, P. Larsson, E. Wallin, M. Lattemann, M. A. Raadu, Ulf Helmersson, Plasma Sources Sci. Technol. **18**, 045008 (2009).
[7] M. Ganciu, S. Konstantinidis, Y. Paint, J. P. Dauchot, M. Hecq, L. de Poucques, P. Vašina, M. Meško, J. C. Imbert, J. Bretagne, M. Touzeau, J. Optoelectron. Adv. Mater. **7**, 2481 (2005).
[8] M. E. McHenry, D. E. Laughlin, Prog. Mater. Sci. 44, 291 (1999).
[9] G. Herzer, Handbook of Magnetic Materials, K.H.J. Buschow (Ed.), **10**, chapter 3, p. 415, Elsevier Science, Amsterdam (1997).
[10] I. L. Velicu, M. Kowalczyk, M. Neagu, V. Tiron, H. Chiriac, J. Ferenc, Mat. Sci. Eng. B-Solid **178**, 1329 (2013).
[11] I. L. Velicu, V. Tiron, G. Popa, Surf. Coat. Tech. http://dx.doi.org/10.1016/j.surfcoat.2014.03.015
[12] T. Gehren, K. Butler, L. Mashonkina, J. Reetz, J. Shi, Astron. Astrophys. **366**, 981 (2001).
[13] G. Nave, S. Johansson, R. C. M. Learner, A. P. Thorne, J. W. Brault, (1994) NIST, Atomic Spectra Database.
[14] W. Demtröder, Laserspektroskopie, Springer, Berlin (2000).
[15] C. Vitelaru, L. de Poucques, T. M. Minea, G. Popa, Plasma Sources Sci. Technol. **20**, 045020 (2011).
[16] C. Vitelaru, L. de Poucques, T. M. Minea, G. Popa, J. Appl. Phys. **109**, 053307 (2011).
[17] C. Vitelaru, T. Minea, L. de Poucques, M. Ganciu, G. Popa, Rom. Journ. Phys. **56**, 47 (2011).
[18] A. Mishra, P. J. Kelly, J. W. Bradley, Plasma Sources Sci. Technol. **19**, 045014 (2010).
[19] K. Macák, V. Kouznetzov, J. M. Schneider, U. Helmersson, I. Petrov, J. Vac. Sci. Technol. A **18**, 1533 (2000).
[20] D. Lundin, P. Larsson, E. Wallin, M. Lattemann, N. Brenning, U. Helmersson, Plasma Sources Sci. Technol. **17**, 035021 (2008).
[21] P. Poolcharuansin, B. Liebig, J. W. Bradley, Plasma Sources Sci. Technol. **21**, 015001 (2012).
[22] J. Alami, J. T. Gudmundsson, J. Bohlmark, J. Birch, Plasma Sources Sci. Technol. **14**, 525 (2005).
[23] K. B. Gylfason, J. Alami, U. Helmersson, J. T. Gudmundsson, J. Phys. D: Appl. Phys. **38**, 3417 (2005).
[24] O. Ishihara, I. Alexeff, H. J. Doucet, W. D. Jones, Phys. Fluids **21**, 2211 (1978).
[25] A. P Ehiasarian, J. Andersson,A. Anders, J. Phys D: Appl. Phys. **43**, 275204 (2010).
[26] D. Bohm, Minimum ionic kinetic energy for a stable sheath, in The Characteristics of Electrical Discharges in Magnetic Field, edited by A. Guthrie and R. K. Wakerling, McGraw-Hill, New York, (1949), p. 77.
[27] J. D. Swift, M. J. R. Schwar, Electrical Probes for Plasma Diagnostics, Iliffe, London, (1970).